Demixing Kinetics in a Binary Polymer Mixture of Poly(methyl methacrylate) and Poly(acrylonitrile-*co*-styrene)

Junko Maruta, Takashi Ohnaga, and Takashi Inoue*

Department of Organic and Polymeric Materials, Tokyo Institute of Technology, Ookayama, Meguro-ku, Tokyo 152, Japan

Received March 23, 1993; Revised Manuscript Received August 24, 1993®

ABSTRACT: Demixing kinetics in a mixture of poly(methyl methacrylate) and poly(acrylonitrile-*co*-styrene) was investigated by time-resolved light scattering during isothermal spinodal decomposition (SD) after a temperature jump from the single-phase region to the two-phase region above the lower critical solution temperature. Two linear regimes were found; i.e., scattered intensity increased exponentially at first and then another exponential increase was observed. When the kinetics were analyzed in more detail on the basis of the linearized theory of SD, the first regime was assigned to the early stage of SD, while the second one was apparent. Numerical calculation with a Cahn–Hilliard type nonlinear diffusion equation revealed that the apparent linear regime accidentally appeared for a system with particular sets of kinetic parameters. The late stage of demixing was well described by the recent scaling theories; time evolution of the scaled wavenumbers of dominant Fourier components in concentration fluctuations yielded a master curve, and a universal scaled structure function was seen.

Introduction

About 20 years ago, McMaster undertook a preliminary study on the spinodal decomposition (SD) of a polymer–polymer mixture.[1] He discussed the demixing behavior of the poly(methyl methacrylate) (PMMA)/poly(acrylonitrile-*co*-styrene) (SAN) mixture on the basis of electron microscopic observation. In these 20 years, there has been great progress in the theoretical aspects of SD. Now we pay attention again to the PMMA/SAN system, since this system offers a unique opportunity for kinetic experimentation. First, both PMMA and SAN have essentially the same T_g (glass transition temperature) so that there is no serious mismatch in mobility factors even at temperatures just above T_g. Second, by changing the acrylonitrile content of SAN, the LCST (lower critical solution temperature) can be adjusted to locate not far above T_g; hence one can precisely measure the kinetic variables for the slow rate process. In this study, we investigate the slow demixing behavior in a PMMA/SAN mixture by time-resolved light scattering. The early, intermediate, and late stages of SD are analyzed by the linearized theory and recent scaling theories.

Experimental Section

The PMMA used was a commercial polymer, Acrypet M001, Mitsubishi Rayon Co. Ltd. ($\bar{M}_n$ = 50 000, $\bar{M}_w$ = 110 000). SAN was kindly supplied by Dr. Y. Aoki, Mitsubishi Chemical Co. Ltd. (AN content = 32.8 wt %, $\bar{M}_w$ = 63 000). PMMA and SAN were dissolved at 7 wt % of total polymer in tetrahydrofuran. After the solvent was evaporated at 15 °C, the cast film was further dried under vacuum of 10^{-4} mmHg at 15 °C for 48 h and at 74 °C for 24 h. The blend specimen thus prepared was clear and transparent.

The phase diagram was determined by the cloud point method employing very long isothermal annealing (up to 48 h).[2]

For the kinetic studies of demixing, the blend film (50/50 PMMA/SAN) was annealed at 130 °C (in the single-phase region) for 30 min in a hot chamber and then inserted into another hot chamber kept at a constant temperature in the two-phase region (149, 159, 163, 167, and 175 °C). During isothermal annealing, a He–Ne laser of 632.8-nm wavelength was applied vertically to the film specimen and the goniometer trace of the intensity of the scattered light was given at appropriate intervals.

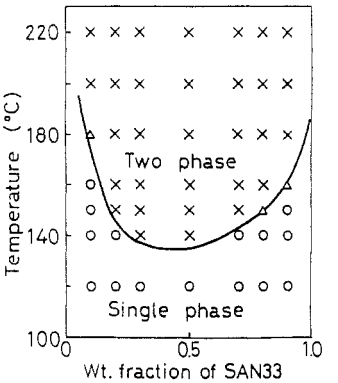

Figure 1. Phase diagram of the PMMA/SAN system: (×) cloudy film and irregular two-phase morphology observed under the light microscopy; (○) clear film; (△) the × judgement after 10 h of annealing changed to the ○ one after further 38 h of annealing.

Results and Discussion

Phase Diagram and Scattering Profile. In Figure 1 is shown the phase diagram of the PMMA/SAN system. LCST type phase behavior is seen, as reported by McMaster.[1] The T_g's of PMMA and SAN are about 100 °C, and the LCST (~135 °C) locates not far above T_g. Therefore slow phase demixing is expected to be observed in the two-phase region.

Figure 2 shows the time variation of scattered intensity $I(q,t)$ for the 50/50 mixture after the temperature jump from 130 to 159 °C. The scattering profile has no peak in the measured q range at the initial stage of demixing. The peak appears at t = 276 min (Figure 2a). The peak angle remains constant, and the scattering intensity increases with time for a while, and then the peak position shifts to lower q after t = 390 min (Figure 2b,c). This time variation of the light scattering profile is characteristic of SD.

Early Stage. First, we analyze the initial stage by the linearized theory of Cahn.[3,4] The theory for the early stage of SD predicts an exponential growth of the scattering intensity $I(q)$ ($\sim S(q,t)$; $S(q,t)$ being the structure function) with time t as expressed in eq 1 for $q < q_c$ (q_c being the upper critical wavenumber) and the presence of the fastest

* To whom correspondence should be addressed.
® Abstract published in *Advance ACS Abstracts*, October 15, 1993.

0024-9297/93/2226-6386$04.00/0

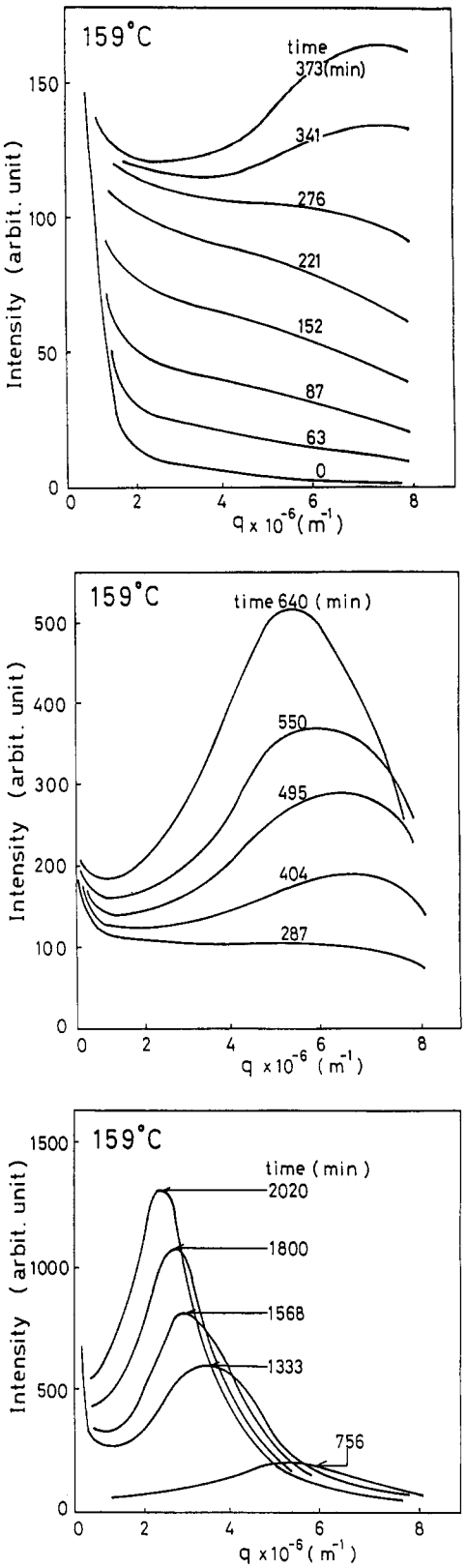

Figure 2. Change of light scattering profile with annealing at 159 °C (50/50 PMMA/SAN): (a, top) early stage, (b, middle) intermediate-to-late stage, and (c, bottom) late stage. Numbers give the annealing time after temperature jump.

growth at a time-independent wavenumber $q_m = q_c/2^{1/2}$

$$S(q,t) = S(q,0)\exp\{2R(q)t\} \quad (1)$$

$$R(q) = -Mq^2\left(\frac{\partial^2 f}{\partial c^2} + 2\kappa q^2\right) \quad (2)$$

where M is the diffusion mobility, f is the free energy density, c is the concentration, κ is the energy gradient

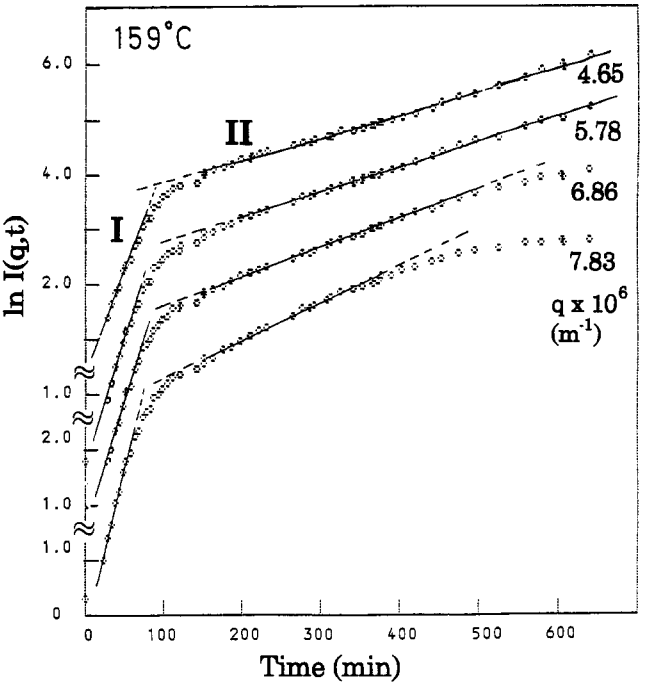

Figure 3. Change of the scattered intensity at various q's with time after the temperature jump from 135 to 159 °C by a ln plot (50/50 PMMA/SAN).

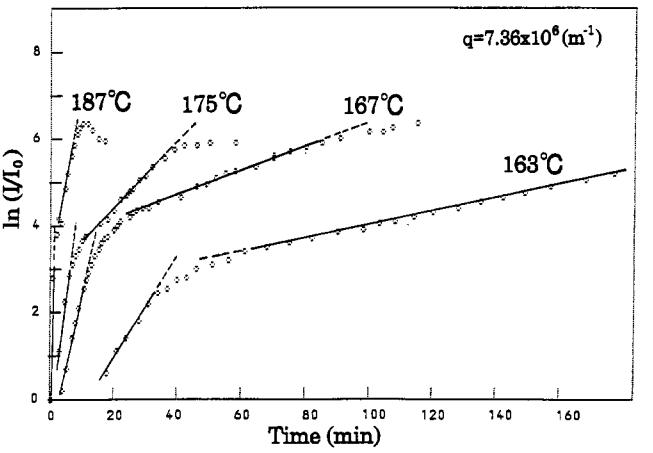

Figure 4. Change of the scattered intensity of $q = 7.36 \times 10^6$ m^{-1} at various temperatures (187, 175, 167, and 163 °C).

coefficient, and q is the wave vector. $R(q)$ is the amplification factor which describes the growth rate of concentration fluctuation with wavenumber q. In Figure 3 is shown the ln $I(q,t)$ vs t plot according to eq 1. There are two different linear regimes I and II. The linear regimes are maintained for a long period. Such two linear regimes are observed at various temperatures as shown in Figure 4. In the literature, one can find two similar linear regimes for a mixture of perdeuterated and protonated 1,4-polybutadienes by Bates.[5] Cahn's theory has been modified to incorporate the effect of a flux arising from the random thermal motion of the molecules in addition to the flux produced by the composition gradient.[6] Then $S(q,t)$ has been rewritten in the context of Cahn's theory:

$$S(q,t) = S(q,\infty) + [S(q,0) - S(q,\infty)]\exp\{2R(q)t\} \quad (3)$$

where $S(q,\infty)$ is the so-called virtual structure factor defined as

$$S(q,\infty) = -Mk_BTq^2/R(q) \quad k_B\text{: Boltzmann constant} \quad (4)$$

Although $S(q,\infty)$ can be determined by nonlinear fitting of eq 3 to the scattering data and $R(q)$ is obtained,[7] this nonlinear fitting depends on the time range. One can easily

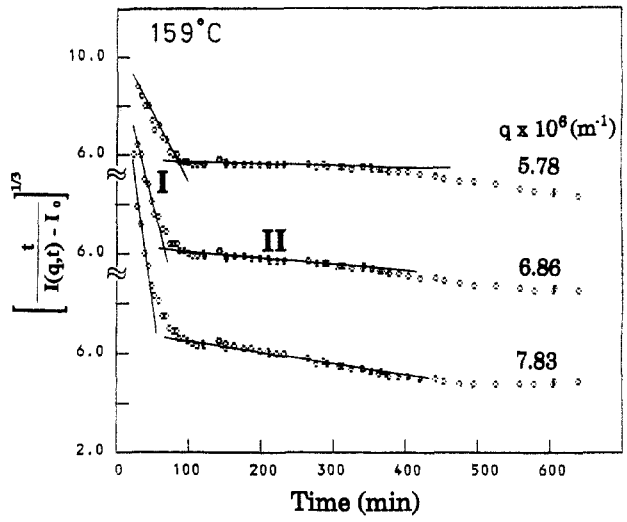

Figure 5. 1/3 power plot of the data in Figure 3.

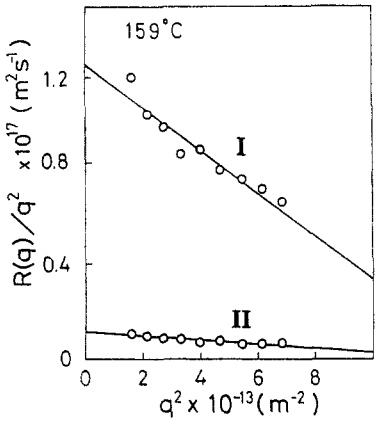

Figure 6. Plots of $R(q)/q^2$ vs q^2 from the data in Figure 3.

estimate $R(q)$ by the 1/3 power plot proposed by Sato and Han:[8]

$$\left[\frac{t}{I(q,t)-I_0}\right]^{1/3} = \frac{1}{[2(I_0-I_\infty)R(q)]^{1/3}}\left\{1-\frac{1}{3}R(q)t+\frac{1}{81}[R(q)t]^3+\ldots\right\} \quad (5)$$

where $I_\infty = KS_\infty + I_b$ and $I_0 = KS_0 + I_b$ (I_b being the background intensity and K a constant). In Figure 5 is shown the plot based on eq 5. Two linear regimes are also seen in this plot. Note that the prerequisite $R(q)t < 1$ for the 1/3 power plot is satisfied for both regimes. One may apply Cahn's linearized theory to interpret the first linear regime. However, the problem is why another linear regime appears. To answer the question, we further extend the analysis following the linearized theory.

$R(q)/q^2$ vs q^2 plots based on eq 2 are given in Figures 6 and 7 from the results of Figures 3 and 5, respectively. The slopes of stage I in both figures are negative, while a slope of stage II in Figure 7 is positive. The positive slope is not conceivable from eq 2. It may suggest that the second linear regime is not the real linear regime in a sense of Cahn's theory. The appearance of the second linear regime will be discussed in next section. Following eq 2, D_{app} ($=M\partial^2 f/\partial c^2$) and q_c are determined to be $D_{app} = 1.26 \times 10^{-17}$ m²/s and $q_c = 1.17 \times 10^7$ m⁻¹ for regime I in Figure 6 and $D_{app} = 1.20 \times 10^{-17}$ m²/s and $q_c = 1.39 \times 10^7$ m⁻¹ for regime I in Figure 7. The most probable wavelength Λ_m ($=2\pi/q_m$) are 0.76 μm by the semilog plot and 0.64 μm by the 1/3 power plot. Thus, one sees that the noise term plays quite a minor effect. This may be partly due to our experimental condition of $q \ll q_c$.[7]

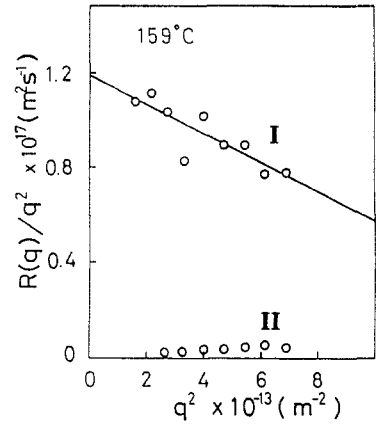

Figure 7. Plots of $R(q)/q^2$ vs q^2 from the data in Figure 5.

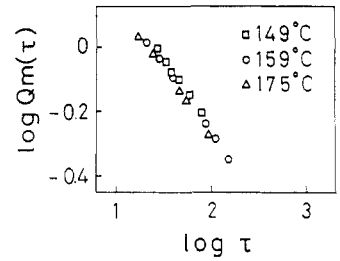

Figure 8. Reduced wavenumber Q_m as a function of reduced time τ.

Late Stage. At the intermediate-to-late stages, time variation of q_m and the scattered intensity at q_m are described in the scaling relations

$$q_m(t) \sim t^{-\alpha} \quad (6)$$

$$i_m(t) \sim t^{\beta} \quad (7)$$

The reduced wavenumber $Q_m(\tau)$ and the reduced scattered intensity $I_m(\tau)$ are defined by Hashimoto et al.[9] for polymer–polymer mixtures as

$$Q_m(\tau) = q_m(\tau)/q_m(\tau=0) \quad (8)$$

$$I_m(\tau) = i_m(\tau)q_m^3(\tau=0)/\int x^2F(x)\,dx \quad (9)$$

where $\xi = 1/q_m$, $t_c = \xi^2/D_{app}$, $\tau = t/t_c$, $F(x) = I(q,t)q_m^3(t)$, and $x = q(t)/q_m(t)$. The reduced variables observed at various temperatures are expected to yield a single master curve as

$$Q_m(\tau) \sim \tau^{-\alpha} \quad (10)$$

$$I_m(\tau) \sim \tau^{\beta} \quad (11)$$

Experimentally, it was shown that $\beta > 3\alpha$ for the intermediate stage and $\beta = 3\alpha$ for the late stage. In Figure 8 are shown the results of scaling analysis for the late stage of SD. The reduced plots for Q_m and τ at various temperatures yield master curves, respectively. For the more comprehensive discussion, Furukawa proposed that $S(q,t)$ is scaled by $q_m(t)$ as[10]

$$S(q,t) \sim q_m^{-d}F(x) \quad (12)$$

where $x = q(t)/q_m(t)$. $F(x)$ is a universal scaling function:

$$F(x) \sim x^2/(\gamma/2 + x^{2+\gamma}) \quad (13)$$

where $\gamma = d + 1$ (for the off-critical mixture) or $\gamma = 2d$ (for the critical mixture). The scaled structure function $F(x)$ obtained experimentally by $F(x) = I(q,t)q_m^3(t)$ is

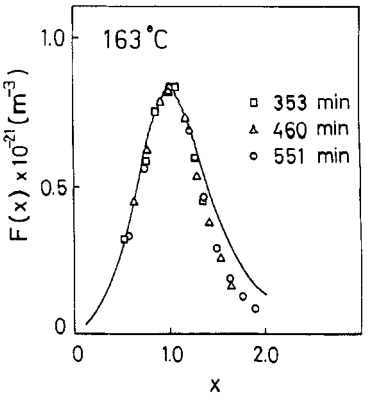

Figure 9. The scaled structure function $F(x)$ determined at 163 °C.

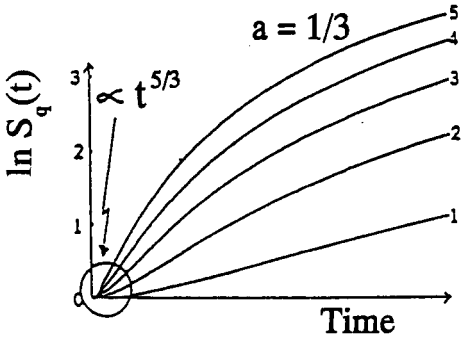

Figure 10. Time evolution of the structure function $S_q(t)$ at the initial stage of demixing, predicted by Furukawa.[10]

shown in Figure 9. The $F(x)$'s at various demixing times overlap with each other, and a universal function exists; however, the experimental function is rather narrower than the theoretical one (solid line in Figure 9) predicted by eq 13. A similar universal function was also found at other temperatures. In this way, the scaling assumption seems to be valid for the late stage of demixing in PMMA/SAN.

Intermediate Stage. Thus, both early and late stages are soundly interpreted by the current theories of SD. An unsolved problem is on the second linear regime at the intermediate stage.

The dynamic scaling theory by Furukawa[10] covers the whole range of SD, i.e., early-to-late stages. The equation of motion for structure function is given by

$$\partial S_q(t)/\partial t = 2Mq^2[k_BT - \{R^d(t)X(qR(t))\}^{-1}S_q(t)] \quad (14)$$

where $R(t) \propto t^{1/(d+2)}$, $S_q(t) = R(t)^dS(qR(t))$, and $X^{-1}(t) = R(t)^{-d}[\alpha + \beta(qR(t))^{d+1}]$. Cahn's theory is described in

$$\partial S_q(t)/\partial t = 2Mq^2[k_BT - (a + Kq^2)S_q(t)] \quad a, K: \text{ constant} \quad (15)$$

Furukawa formulated the initial stage by

$$S_q(t) = 1 + R(t)^dS(qR(t)) \quad (16)$$

$$R(t) = (Ct + 1)^a \quad C: \text{ constant} \quad (17)$$

A series of theoretical plots of $\ln S_q(t)$ vs t according to eqs 16 and 17 is reproduced in Figure 10. Strictly speaking, no linear regime is seen in Figure 10. However, there exists a possibility to find a case in which the $\ln S_q(t)$ curve is roughly approximated by two straight lines, e.g., case 5 in Figure 10. This encourages us to discuss the appearance of the second linear regime. Unfortunately, the dynamic scaling argument itself is too comprehensive to discuss in relation to the molecular and thermodynamic variables. We prefer a computer simulation by the Cahn–Hilliard nonlinear diffusion equation which may adequately describe the intermediate stage.

The detail of the simulation procedure was presented in our previous article.[11] The subject is to describe the concentration fluctuation on the basis of the nonlinear diffusion equation.

$$\frac{\partial c}{\partial t} = \frac{\partial}{\partial x}\left(D\frac{\partial c}{\partial x}\right) - 2M\kappa\left(\frac{\partial^4 c}{\partial x^4}\right) \quad (18)$$

D is a diffusion coefficient defined as

$$D = M\left(\frac{\partial^2 f}{\partial c^2}\right) \quad (19)$$

It should be noted that since $\partial D/\partial x$ is defined by $M(\partial c/\partial x)(\partial^3 f/\partial c^3)$, eq 18 is rewritten as

$$\frac{\partial c}{\partial t} = M\left[\frac{\partial^2 f}{\partial c^2}\left(\frac{\partial^2 c}{\partial x^2}\right) + \frac{\partial^3 f}{\partial c^3}\left(\frac{\partial c}{\partial x}\right)^2 - 2\kappa\left(\frac{\partial^4 c}{\partial x^4}\right)\right] \quad (20)$$

For our numerical calculations, f must be expressed in a polynomial form.

$$f(c) = a_nc^n + a_{n-1}c^{n-1} + ... + a_1c + a_0 \quad (21)$$

D is also expressed in a polynomial form with concentration fluctuation $p = c - c_a$.

$$D(p) = D_mp^m + D_{m-1}p^{m-1} + ... + D_1p + D_0 \quad (22)$$

where c_a is an average concentration. Since the relationship between D and f is given by eq 19, D_i's can be expressed with a_j's.

In order to solve eq 18, the concentration fluctuation p must be expressed as a sum of Fourier series.

$$p(x,t) = \sum_h Q_h \exp\{2\pi xi/(L/h)\} \quad (23)$$

L is the longest wavelength of a Fourier component in a demixing system and Q_h is an amplitude of a Fourier wave with wavelength $L/|h|$ ($h = \pm1, \pm2, ..., h \neq 0$). An equation describing time evolution of an amplitude Q_h of every Fourier waves is given by inserting eqs 22 and 23 into eq 18.

$$\frac{\partial Q_h}{\partial t} = -(hb)^2\{(D_0 + 2h^2b^2M\kappa)Q_h + (1/2)D_1R_h + (1/3)D_2S_h + (1/4)D_3T_h + (1/5)D_4U_h\} \quad (24)$$

where $b = 2\pi/L$, $R_h = \int_{-\infty}^{+\infty}Q_kQ_{h-k}\,dk$, $S_h = \int_{-\infty}^{+\infty}R_kQ_{h-k}\,dk$, $T_h = \int_{-\infty}^{+\infty}S_kQ_{h-k}\,dk$, and $U_h = \int_{-\infty}^{+\infty}T_kQ_{h-k}\,dk$. We used $n = 6$ and $m = 4$ for a numerical calculation. Time evolution of Q_h is calculated as follows.

$$Q_h(t + \Delta t) = Q_h(t) + \left(\frac{\partial Q_h}{\partial t}\right)\Delta t \quad (25)$$

The concentration fluctuation at the time therefore can be obtained by eq 23.

As for the free energy function $f(c)$, we use the Flory–Huggins equation. The temperature dependence of the interaction parameter χ is described by the equation-of-state theory. The Flory–Huggins equation can be approximated in a polynomial form by the least squares method and the coefficients a_i are obtained. D_i's in eq 24 are thus calculated with a_i's.

Time evolution of the scattered intensity $I(q,t)$ is given by

$$I(q,t) = CQ_h(t)^2 \quad C: \text{ constant} \quad (26)$$

where $q = 2\pi h/L$.

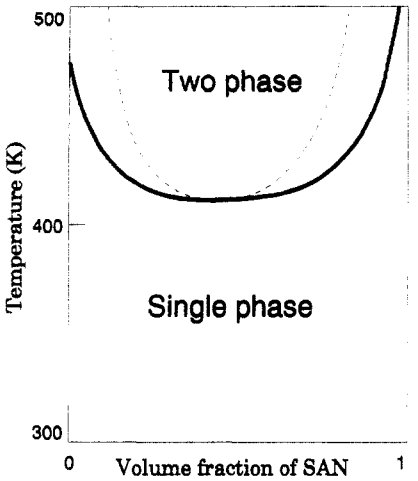

Figure 11. Phase diagram calculated for the PMMA/SAN system: (—) binodal, (- - -) spinodal. The equation-of-state parameters used are $V_1^* = 200\,000$ cm^3/mol, $V_2^* = 110\,000$ cm^3/mol, $T_1^* = 8800$ K, $T_2^* = 8119$ K, $P_1^* = 500$ J/cm^3, and $X_{12} = -0.3$. The thermal expansion coefficients are $\alpha_1 = 4.88 \times 10^{-4}$ K^{-1} and $\alpha_2 = 5.75 \times 10^{-4}$ K^{-1}.

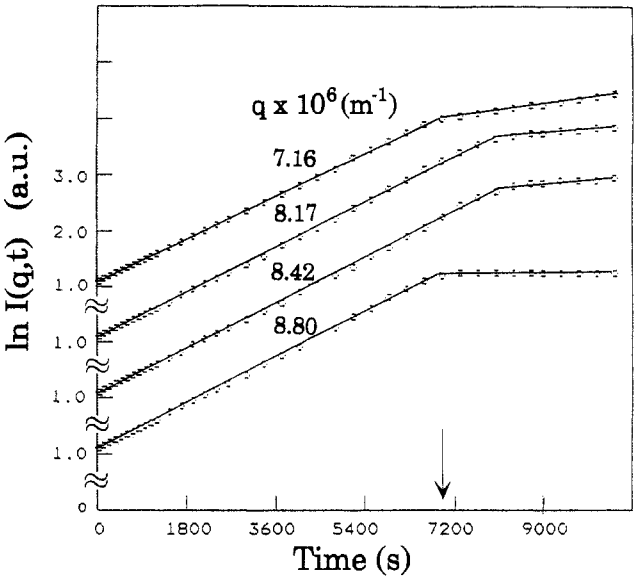

Figure 12. Plot of ln $I(q,t)$ vs t at 159 °C calculated with the Cahn–Hilliard type nonlinear diffusion equation. The kinetic parameters used are $D_0 = 1.20 \times 10^{-17}$ m^2/s and $M\kappa = 3.11 \times 10^{-32}$ m^4/s.

We performed the computer simulation on the demixing caused by a temperature jump from a single-phase region to a two-phase region. In Figure 11 is shown a phase diagram used in this calculation. The simulation result is shown in Figure 12. The two linear regimes are realized at various q's. Thus, we can successfully justify the presence of the two linear regimes. Note that after the crossover time, $t = 6960$ s for $q = 8.80 \times 10^6$ m^{-1}, e.g., shown by the arrow in Figure 12, q_m started to shift to the lower q. It means that the second linear regime is caused by the nonlinear terms and is out of the early stage of SD. Now, the problem is why it yields the straight line. In Figure 13 are shown the results of similar plots for the various sets of values of κ, $a_0 \sim a_6$, and D_0. Curve a is for the same set as in Figure 12. Curve b is obtained when κ is replaced by 0.5κ. Curve c is calculated when D_0 is replaced by $2.5D_0$ and a_2 by $0.98a_2$. Both curves b and c

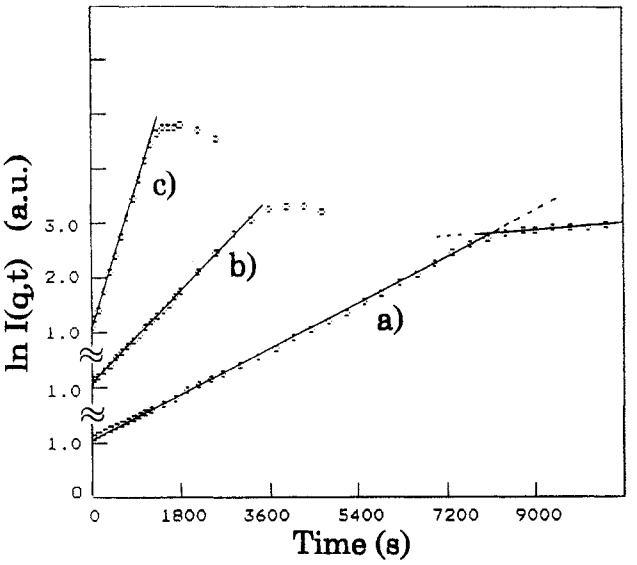

Figure 13. Plot of ln $I(q,t)$ vs t at 159 °C calculated with the Cahn–Hilliard type nonlinear diffusion equation. Calculation was done under the same condition as in Figure 12. The parameters were changed as follows; (a) → (b), $\kappa \rightarrow 0.5\kappa$; (b) → (c), $D_0 \rightarrow 2.5D_0$, $a_2 \rightarrow 0.98a_2$.

have the single linear regime. It means that the second linear regime appears only for a particular set of values of κ, $a_0 \sim a_6$, and D_0.

Conclusion

Demixing kinetics in a binary polymer mixture of PMMA and SAN was investigated by time-resolved light scattering. A linear regime described by Cahn's theory was found to exist at the initial stage of demixing. Another linear regime was observed at the intermediate stage. A computer simulation on demixing using the Cahn–Hilliard type nonlinear diffusion equation revealed that the second linearity occurs accidentally for the particular set of values of the energy gradient coefficient, the second derivative of the free energy with respect to concentration, and the chain mobility. The late stage was successfully described by the scaling rule. Many experimental studies have suggested that the demixing behavior in the late stage of SD had universality,[9,12-16] and our results were in accordance with the conclusion in the previous studies.

References and Notes

(1) McMaster, L. P. *Adv. Chem. Ser.* **1975**, *142*, 43.
(2) Maruta, J.; Ougizawa, T.; Inoue, T. *Polymer* **1988**, *29*, 2056.
(3) Cahn, J. W. *J. Phys. Chem.* **1965**, *42*, 93.
(4) Cahn, J. W.; Hilliard, J. E. *J. Chem. Phys.* **1958**, *28*, 258.
(5) Bates, F. S.; Wiltzius, P. *J. Chem. Phys.* **1989**, *91*, 3258.
(6) Cook, H. E. *Acta Metall.* **1970**, *18*, 297.
(7) Okada, M.; Han, C. C. *J. Chem. Phys.* **1986**, *85*, 5317.
(8) Sato, T.; Han, C. C. *J. Chem. Phys.* **1988**, *88*, 2057.
(9) Hashimoto, T.; Itakura, M.; Shimidzu, N. *J. Chem. Phys.* **1986**, *85*, 6773.
(10) Furukawa, H. *Physica A* **1987**, *A123*, 497.
(11) Ohnaga, T.; Inoue, T. *J. Polym. Sci., Polym. Phys. Ed.* **1989**, *27*, 1675.
(12) Takenaka, M.; Izumitani, T.; Hashimoto, T. *J. Chem. Phys.* **1990**, *92*, 4566.
(13) Takenaka, M.; Izumitani, T.; Hashimoto, T. *J. Chem. Phys.* **1992**, *97*, 6855.
(14) Hashimoto, T.; Itakura, M.; Hasegawa, H. *J. Chem. Phys.* **1986**, *85*, 6118.
(15) Song, M.; Huang, Y.; Cong, G.; Liang, H.; Jiang, B. *Polymer* **1992**, *33*, 1293.
(16) Kyu, T.; Lim, D. S. *Macromolecules* **1991**, *24*, 3645.